Inorganic Chemistry

Article

pubs.acs.org/IC

Molecular and Electronic Structures of the Members of the Electron Transfer Series $[Mn(bpy)_3]^n$ (n = 2+, 1+, 0, 1−) and $[Mn(tpy)_2]^m$ (m = 4+, 3+, 2+, 1+, 0). An Experimental and Density Functional Theory Study

Mei Wang,‡ Jason England,‡ Thomas Weyhermüller, and Karl Wieghardt*

Max Planck Institute for Chemical Energy Conversion, Stiftstrasse 34−36, D-45470 Mülheim an der Ruhr, Germany

Supporting Information

ABSTRACT: The members of the electron transfer series $[Mn(bpy)_3]^n$ (n = 2+, 1+, 0, 1−) and $[Mn(tpy)_2]^m$ (m = 2+, 1+, 0) have been investigated using a combination of magnetochemistry, electrochemistry, and UV−vis−NIR spectroscopy; and X-ray crystal structures of $[Mn^{II}(^{Me}bpy^{\bullet})_2(^{Me}bpy^0)]^0$, $[Li(THF)_4][Mn^{II}(bpy^{\bullet})_3]$, and $[Mn^{II}(tpy^{\bullet})_2]^0$ have been obtained (bpy = 2,2′-bipyridine; ^{Me}bpy = 4,4′-dimethyl-2,2′-bipyridine; tpy = 2,2′:6,2″-terpyridine; THF = tetrahydrofuran). It is the first time that the latter complex has been isolated and characterized. Through these studies, the electronic structures of each member of both series of complexes have been elucidated, and their molecular and electronic structures further corroborated by broken symmetry (BS) density functional theoretical (DFT) calculations. It is shown that all one-electron reductions that comprise the aforementioned redox series are ligand-based. Hence, all species contain a central high-spin Mn^{II} ion (S_{Mn} = 5/2). In contrast, the analogous series of Tc^{II} and Re^{II} complexes possess low-spin electron configurations.

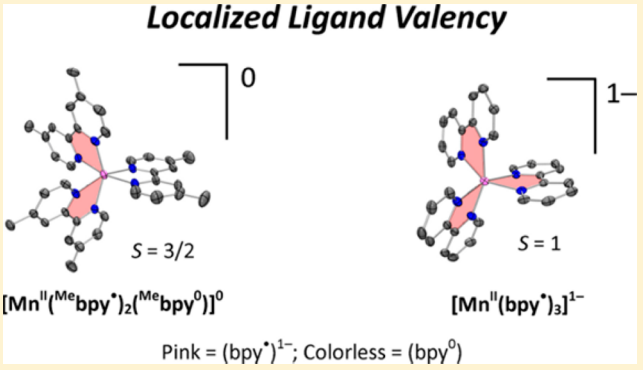

INTRODUCTION

Octahedral tris(2,2′-bipyridine) and bis(2,2′:6,2″-terpyridine) complexes are known for all transition metals, and they frequently form electron transfer series $[M(bpy)_3]^n$ and $[M(tpy)_2]^m$ (bpy = 2,2′-bipyridine; tpy = 2,2′:6,2″-terpyridine) in which their charges (n and m) can, in principle, range from 4+ (in a few cases) to 3−, thereby yielding up to seven (or eight) individual species.[1] This has already been demonstrated for $[Cr^{III}(bpy)^3]^n$ (n = 3+ to 3−) and $[Cr^{III}(tpy)_2]^m$ (m = 3+ to 1−).[2,3] The electronic structure of a given species is determined by the d^N electron configuration at the central metal ion (its oxidation state), which can vary in a given series, and the redox state of the individual bpy or tpy ligands, which are now recognized to bind either as diamagnetic neutral $(bpy^0)/(tpy^0)$ ligands, as π-radical monoanions $(bpy^{\bullet})^{1-}/(tpy^{\bullet})^{1-}$, or as diamagnetic dianions $(bpy^{2-})^{2-}/(tpy^{2-})^{2-}$.[4,5] In other words, bpy and tpy are redox-active (noninnocent) ligands.

Herein, we report our efforts to clarify the electronic structures of the series of group 7 transition metal ion complexes $[M(bpy)_3]^n$ and $[M(tpy)_2]^m$ (M = Mn, Tc, Re; n = 2+, 1+, 0, 1−; m = 2+, 1+, 0). The previously isolated and characterized members of these series are summarized in Chart 1.[6−20] Note that the strongly reduced species $Na_4[Mn(bpy)_3]\cdot 3THF\cdot 5$(1,4-dioxane) has also been reported.[12a] Here we prepared the neutral complexes $[Mn(^{Me}bpy)_3]^0$ (^{Me}bpy =4,4′-dimethyl-2,2′-bipyridine) and $[Mn(tpy)_2]^0$ for the first time.

RESULTS AND DISCUSSION

The $[Mn(bpy)_3]^n$ (n = 2+, 1+, 0, 1−) Series. It is well established that the colorless dication $[Mn^{II}(bpy^0)_3]^{2+}$ (S = 5/2) contains a high-spin $3d^5$ central manganese(II) ion and three neutral N,N'-coordinated bpy ligands. In the potential range of 0 to −2.5 V vs the ferricenium/ferrocene redox couple (Fc^+/Fc), this species can undergo three successive reversible one-electron reductions (Table 1)[21] to sequentially yield an unstable monocation, a stable neutral species, and a stable but highly oxygen sensitive monoanion, which possess S = 2, 3/2, and 1 electronic ground states, respectively.[6−12,18−21] With the exception of the monocation $[Mn(bpy)_3]^{1+}$, which is unstable in solution due to either disproportionation or loss of a coordinated neutral (bpy^0) ligand, all the other species have been isolated as solid materials (Chart 1). In addition, Herzog and Grimm[12a] have reported the synthesis of black crystals of the complex $Na_4[Mn(bpy)_3]\cdot 3THF\cdot 5$(1,4-dioxane), which possesses an S = 5/2 ground state, via reduction of the neutral species $[Mn(bpy)_3]^0$ in THF solution using sodium metal.

In an effort to obtain single crystals suitable for X-ray crystallography, the neutral complex $[Mn(^{Me}bpy)_3]^0$ was prepared by reaction of 3 equiv of neutral ligand with 1 equiv of $MnBr_2$ and 2 equiv of sodium amalgam in anhydrous

Received: December 4, 2013
Published: January 27, 2014

   dx.doi.org/10.1021/ic4029854 | Inorg. Chem. 2014, 53, 2276−2287

Chart 1. Synthesis, Magnetism and X-ray Structures of $[M(bpy)_3]^n$ and $[M(tpy)_2]^{m a}$

Complex[a]	Synthesis and Properties Ref.	Ground State (S)	X-Ray Structure Ref.
$[Mn(bpy)_3]^{2+}$	6,8	5/2	7
$[Mn(bpy)_3]^{0}$	9,10	3/2	not known
$[Mn(^{Me}bpy)_3]^{0}$	this work	3/2	this work
$[Mn(bpy)_3]^{1-}$	10,11	1	this work
$[Mn(bpy)_3]^{4-}$	12	5/2	not known
$[Tc(bpy)_3]^{2+}$	13	1/2	13b
$[Re(bpy_3)]^{3+}$	14	not known	not known
$[Re(bpy_3]^{2+}$	15,16	1/2	15
$[Re(bpy)_3]^{1+}$	16	0	16
$[Re(bpy)_3]^{0}$	17	μ_{eff} = 4.0 (300 K)	not known
$[Mn(tpy)_2]^{0}$	this work	3/2	this work
$[Mn(tpy)_2]^{2+}$	18	5/2	18a–d
$[Mn(tpy)_2]^{3+}$	19	2	19
$[Mn(tpy)_2]^{4+}$	20	3/2	not known
$[Tc(tpy)_2]^{2+}$	13	1/2	not known
$[Re(tpy)_2]^{1+}$	16	0	not known

[a]The abbreviations bpy and tpy are used in a generic sense without specifying their oxidation level. When we wish to specify the oxidation level in a complex we use $(bpy^0)/(tpy^0)$ for the diamagnetic neutral ligand, $(bpy^{\bullet})^{1-}/(tpy^{\bullet})^{1-}$ for the π-radical anion, and $(bpy^{2-})^{2-}/(tpy^{2-})^{2-}$ for the diamagnetic dianion. Additionally, ^{Me}bpy = 4,4′-dimethyl-2,2-bipyridine.

THF under strictly anaerobic conditions. From the crude product, single crystals of the target compound were grown as the solvate $[Mn(^{Me}bpy)_3]^0\cdot(n\text{-pentane})\cdot 0.5THF\cdot 0.25(^{Me}bpy)$. Further recrystallization and drying *in vacuo* provided pure $[Mn(^{Me}bpy)_3]^0$.

The electronic spectra of the neutral and monoanionic species $[Mn(bpy)_3]^{0,1-}$ are similar to one another (Table 2 and Figure 1) but starkly different from that of the dication $[Mn(bpy)_3]^{2+}$, which is pale yellow in color and does not possess intense (ε_{max} > 10 M^{-1} cm^{-1}) transitions in the visible region. (The spectrum of the monocation has not been recorded due to its inherent instability in solution.) More specifically, both the neutral species $[Mn(bpy)_3]^0$,[12b] whose spectrum is near identical to that of $[Mn(^{Me}bpy)_3]^0$, and the monoanion $[Mn(bpy)_3]^{1-}$ possess three intense bands ($\varepsilon_{max} \approx 10^4$ M^{-1} cm^{-1}) in the visible and near-infrared region, each of which display vibrational fine structure. These spectral features are indicative of the presence of *N,N′*-coordinated $(bpy^{\bullet})^{1-}$ π-radical anions, as previously observed for $[M(bpy)_3]^{0,1-}$ (M = Fe,[25] Ru[26]), and closely resemble those reported for alkali metal salts of $(bpy^{\bullet})^{1-}$ in 1,4-dioxane solution by König and Kremer in 1970.[24] These authors observed three intense ($\varepsilon_{max} \approx 10^4$ M^{-1} cm^{-1}) bands at ~820, 530, and 385 nm for the π-radical anion $(bpy^{\bullet})^{1-}$ and two intense bands at ~610 and 373 nm for the dianion $(bpy^{2-})^{2-}$.

Table 2. Electronic Spectra of Complexes

complex	λ_{max}, nm (ε_{max}, 10^4 M^{-1} cm^{-1})
$[Mn(bpy)_3]^{0a}$	286 (2.5), 345 sh, 385 (1.4), 526 (0.5), 833 (10.2)
$[Mn(^{Me}bpy)_3]^{0b}$	350 (3.8), 400 (3.1), 495 (1.8), 510 (2.7), 580 sh, 870 sh, 980 (0.9), 1400 (0.25) sh
$[Mn(bpy)_3]^{1-b}$	390 (3.7), 530 (1.5), 750 sh, 815 (0,75), 920 (0.7), 1200 sh (0.3)
$[Mn(tpy)_2]^{0b}$	390 (3.1), 420 sh, 595 (2.1), 700 sh, 890 (0.8), 1724[c], 1923[c], 2634[c]
$[Re(bpy)_3]^{2+d}$	298 (4.3), 398 (1.1), 526 (0.8), 668 (0.9) [302 (1.4), 375 (2.5), 495 (0.2)][e]
$[Re(bpy)_3]^{1+d}$	290 (3.0), 444 (2.0), 506 (1.7), 823 (1.3)
$[Re(tpy)_2]^{1+d}$	206 (3.8), 226 (4.1), 284 (3.3), 314 (3.2), 438 (2.0), 558 (1.1), 706 (1.0)
$[Re(bpy)_2Cl_2]^{1+d}$	296 (0.6), 392 (1.1), 596 (0.9)

[a]References 12b and 21a. [b]This work; spectrum recorded in toluene solution (20 °C). [c]Recorded in the solid-state as a KBr pellet. [d]Reference 16, recorded in CH_3CN solution. [e]Reference 15, recorded in aqueous solution in the presence of O_2.

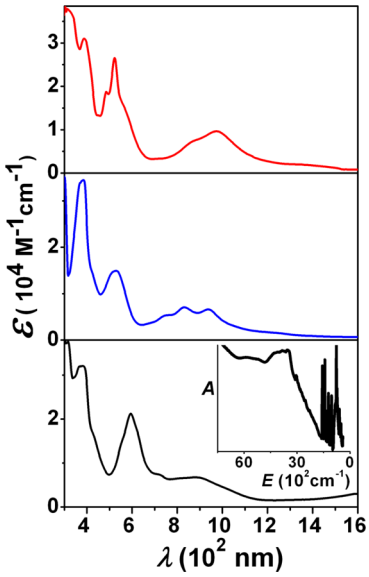

Figure 1. Electronic spectra, recorded in toluene solution at 20 °C, of $[Mn^{II}(^{Me}bpy^{\bullet})_2(^{Me}bpy^0)]^0$ (top), $[Li(THF)_4][Mn^{II}(bpy^{\bullet})_3]^0$ (middle), and $[Mn^{II}(tpy^{\bullet})_2]^0$ (bottom). The inset in the bottom panel contains the near IR spectrum of the latter complex.

Table 1. Redox Potentials ($E_{1/2}$, V vs Fc^+/Fc) of Complexes[a]

complex	solvent	$E^1_{1/2}$(3+/2+)	$E^2_{1/2}$(2+/1+)	$E^3_{1/2}$(1+/0)	$E^4_{1/2}$(0/1−)	ref
$[Fe(bpy)_3]^n$	DMF/AN		−1.66	−1.94	−2.10	22
$[Ru(bpy)_3]^n$	DMF/AN		−1.65	−1.83	−2.08	23
$[Mn(^{Me}bpy)_3]^{nb}$	AN	+1.85[c]	−1.74	−1.92	−2.13	this work
$[Tc(bpy)_3]^n$	AN	*d*	−0.74	−1.76	−2.10	13b
$[Re(bpy)_3]^n$	DMA/acetone	−0.05	−0.83	−1.77	−2.12	16
$[Mn(tpy)_2]^n$	AN	+0.86[e]	−1.52	−1.86	−2.37	20, 21
$[Re(tpy)_2]^n$	DMA		−0.43	−1.97	−2.31	16

[a]Abbreviations: DMF = *N,N*-dimethylformamide, AN = acetonitrile, DMA = *N,N*-dimethylacetamide. [b]Values for $[Mn(bpy)_3]^n$ are similar and given in refs 21 and 22b. [c]Quasi-reversible. [d]Not available. [e]A reversible one-electron redox couple at +1.67 V corresponding to $E_{1/2}$(4+/3+) has been reported.[21]

dx.doi.org/10.1021/ic4029854 | *Inorg. Chem.* 2014, 53, 2276−2287

The magnetic properties (Table 3) of the dication, the neutral, and the monoanionic species have been previously investigated. The dication was found to possess an $S = 5/2$ ground state (high-spin d^5),[18] whereas the neutral species exhibits an $S = 3/2$ ground state, which was proposed to derive from intramolecular antiferromagnetic coupling of the unpaired spins of two $(bpy^{\bullet})^{1-}$ π-radical anions with the five unpaired electrons of the high-spin Mn^{II} ion ($J = -140$ cm^{-1}; eq 1),[10]

$$\hat{H} = -2J \sum_i S_{Mn} \cdot S_i \quad (1)$$

where $S_{Mn} = 5/2$, $S_i = 1/2$, and $i = 1, 2$. Similarly, the monoanion has an $S = 1$ ground state due to intramolecular antiferromagnetic coupling of the spins of three $(bpy^{\bullet})^{1-}$ ligands ($i = 1, 2, 3$) with the five unpaired electrons of the central high-spin Mn^{II} ion ($J = -122$ cm^{-1}).[10] Our own magnetochemical measurements (4–300 K) display excellent agreement with the aforementioned data (Figure 2), thereby confirming the presence of $S = 3/2$ and 1 ground states for $[Mn(^{Me}bpy)_3]^0$ and $[Mn(bpy)_3]^{1-}$, respectively. Although an antiferromagnetic coupling constant of $J = -108 \pm 10$ cm^{-1} was observed for the monoanion, in excellent agreement with the previous measurement,[10] the magnetic moment of $[Mn(^{Me}bpy)_3]^0$ was found to be effectively temperature independent. This suggests that J for the latter complex is less than -200 cm^{-1}. Once again, the monocation has not been experimentally investigated for reasons outlined previously, but it is reasonable to assume that it possesses an $S = 2$ ground state resulting from antiferromagnetic coupling of a high-spin Mn^{II} ion with a single $(bpy^{\bullet})^{1-}$ π-radical. This postulate is corroborated computationally (see below). Inoue et al.[10] have correctly inferred from the above data that "excess electrons are mostly localized in the antibonding π orbitals of bipyridine rather than in the orbitals of manganese." Thus, the electronic structures of this series of complexes are best descibed as $[Mn^{II}(bpy^0)_3]^{2+}$ ($S = 5/2$), $[Mn^{II}(bpy^{\bullet})(bpy^0)_2]^{1+}$ ($S = 2$), $[Mn^{II}(bpy^{\bullet})_2(bpy^0)]^0$ ($S = 3/2$), and $[Mn^{II}(bpy^{\bullet})_3]^{1-}$ ($S = 1$).

Table 3. Experimental and Calculated Magnetic Properties of Complexes

complex	ground state (S)	J_{exptl} (cm^{-1})[a]	J_{calcd} (cm^{-1})[a]	ref
$[Mn^{II}(bpy^0)_3]^{2+}$	5/2			18
$[Mn^{II}(bpy^{\bullet})(bpy^0)_2]^{1+}$	2	[b]	−194 (−197)[c]	this work
$[Mn^{II}(bpy^{\bullet})_2(bpy^0)]^0$	3/2	−140	−156 (−207)[c]	10
$[Mn^{II}(^{Me}bpy)_3]^0$	3/2	<−200		this work
$[Mn^{II}(bpy^{\bullet})_3]^{1-}$	1	−108	−100 (−126)[c]	10
$[Mn^{II}(bpy^{2-})_3]^{4-}$	5/2			12
$[Mn^{II}(tpy^{\bullet})_2]^0$	3/2	<−200	−223 (−247)[d]	this work
$[Tc^{II}(bpy^0)_3]^{2+}$	1/2			27
$[Re^{II}(bpy^0)_3]^{2+}$	1/2			16
$[Re^{II}(bpy^{\bullet})(bpy^0)_2]^{1+}$	0			16

[a]Experimental (exptl) and calculated (calcd) magnetic coupling constants J in cm^{-1} obtained using the spin-Hamiltonian $\hat{H} = -2J\sum_i S_M \cdot S_i$ ($S_i = 1/2$; $i = 1, 2, 3$ (the number of unpaired electrons on the ligands); S_M = local spin at the metal ion). [b]Not measured. [c]Values in parentheses were obtained from single point calculations using geometry optimized structures calculated with inclusion of COSMO for water. [d]Value in parentheses was obtained from a single point calculation using atomic coordinates of an X-ray structure.

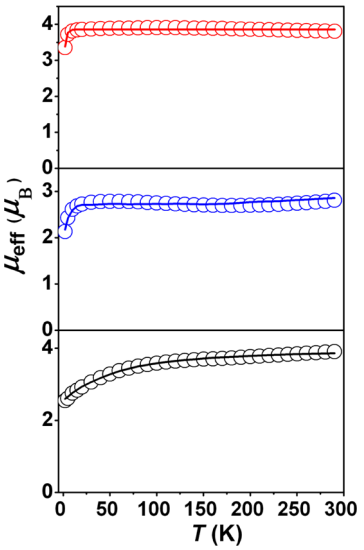

Figure 2. Temperature dependence of the magnetic moments (μ_{eff}) of (top) $S = 3/2$ $[Mn^{II}(^{Me}bpy^{\bullet})_2(^{Me}bpy^0)]^0$ (simulation parameters, $g = 2.0$; $|D| = 0.32$ cm^{-1}; paramagnetic ($S = 5/2$) impurity ~1%), (middle) $S = 1$ $[Li(THF)_4][Mn^{II}(bpy^{\bullet})_3]$ (simulation parameters, $g = 2.0$; $J = 108$ cm^{-1}; $|D| = 0.33$ cm^{-1}), and (bottom) $S = 3/2$ $[Mn^{II}(tpy^{\bullet})_2]^0$ (simulation parameters, $g = 2.0$; $|D| = 1.3$ cm^{-1}; paramagnetic ($S = 5/2$) impurity ~1%). Open circles represent measured data, and solid lines correspond to simulations.

The $[Tc(bpy)_3]^n$ (n = 2+, 1+, 0, 1−) Series. Dilworth et al.[13] have described the preparation of blue-black $[Tc(bpy)_3](PF_6)_2$ in good yield by reaction of $[Tc^{III}Cl_3(CH_3CN)(PPh_3)_2]^0$ with an excess of bpy in dry methanol. The accompanying single crystal X-ray structure of this complex is of relatively good quality and exhibits an average $C_{py}-C_{py}'$ bond distance of 1.482(16) Å that is indicative of three neutral (bpy^0) ligands being present. Additionally, the Tc–N bonds are equivalent and short at 2.077(10) Å, from which a low-spin d^5 Tc^{II} ($S = 1/2$) electron configuration can be inferred. A doublet ground state was later confirmed by EPR spectroscopy.[27] On the basis of the aforementioned data, the electronic structure of $[Tc(bpy)_3](PF_6)_2$ can be assigned as $[Tc^{II}(bpy^0)_3](PF_6)_2$.

The cyclic voltammogram of $[Tc(bpy)_3][BPh_4]_2$, recorded in CH_3CN solution containing 0.2 M $[N(Bu)_4][BF_4]$ electrolyte under a dinitrogen atmosphere, displays three reversible one-electron reduction waves (Table 1). These results show that the monocationic, neutral, and monoanionic species are electrochemically accessible. Although the series $[Tc(bpy)_3]^n$ (n = 2+, 1+, 0, 1−) exists, with the exception of the dication $[Tc^{II}(bpy^0)_3]^{2+}$, none of these species have been isolated or spectroscopically characterized.

The $[Re(bpy)_3]^n$ (n = 2+, 1+, 0, 1−) Series. Bürgi et al.[15] and Harman et al.[16] have reported the synthesis of a few salts containing the dication $[Re^{II}(bpy^0)_3]^{2+}$. For example, $[Re^{II}(bpy^0)_3][ReO_4]_2 \cdot H_2O$ has been structurally characterized, its electronic spectrum in H_2O solution in the presence of O_2 (Table 2) has been recorded, and its effective magnetic moment (μ_{eff}) has been determined to be 1.6 μ_B between 2 and 70 K, which indicates that it possesses a doublet ($S = 1/2$) ground state.[15] Its crystal structure contains three equivalent neutral (bpy^0) ligands and exhibits short Re–N bond lengths; hence the Re center possesses a low-spin $5d^5$ electronic configuration.

dx.doi.org/10.1021/ic4029854 | Inorg. Chem. 2014, 53, 2276–2287

The corresponding monocationic species $[Re(bpy)_3]^{1+}$ has been isolated as a PF_6^- salt, and a rather low-quality X-ray structure was reported, from which little can be concluded except that the Re ion possesses a low-spin ground state.[16] Its electronic spectrum (Table 2) displays features characteristic of at least one $(bpy^\bullet)^{1-}$ π-radical anion being present,[16] and its "normal" ^1H NMR spectrum points to a diamagnetic ground state. Although on the basis of this data its electronic structure cannot be unequivocally assigned, the aforementioned electronic spectrum suggests that $[Re^I(bpy^0)_3]^{1+}$ proposed by the original authors[16] is unlikely. Instead, we favor $[Re^{II}(bpy^\bullet)(bpy^0)_2]^{1+}$, wherein the singlet ground state is obtained by antiferromagnetic coupling of the one unpaired electron at the low-spin Re^{II} ion with that on the single $(bpy^\bullet)^{1-}$ ligand. Neutral $[Re(bpy)_3]^0$ has also been prepared, for which a room temperature magnetic moment of $\mu_{eff} = 4.01$ μ_B was reported.[17] Its molecular and electronic structure has yet to be investigated.

The electrochemistry of $[Re(bpy)_3](PF_6)_2$[16] in CH_3CN solution is remarkably similar to that of $[Tc(bpy)_3](BPh_4)_2$,[13] with three reversible one-electron reduction processes being observed at redox potentials near-identical to those reported for $[Tc(bpy)_3]^{2+}$ (Table 1). In addition, a reversible one electron oxidation wave at +0.10 V (vs Fc^+/Fc), corresponding to eq 2, has been reported for the rhenium complex.

$$[Re^{II}(bpy^0)_3]^{2+} \underset{+e^-}{\overset{-e^-}{\rightleftharpoons}} [Re^{III}(bpy^0)_3]^{3+} \quad (2)$$

Thus, the complete five-membered series $[Re(bpy)_3]^n$ (n = 3+, 2+, 1+, 0, 1−) is electrochemically accessible. Although a solid claimed to be $[Re(bpy)_3]Cl_3$ and displaying a magnetic moment of 1.0 μ_B at 295 K has been reported,[14] further spectroscopic characterization is required to confirm its identity and assign its electronic structure. Even less information is available for the monoanion, with no material isolated or spectroscopic information reported thus far.

Interestingly, Harmann et al.[16] have also reported the synthesis of the paramagnetic complex *cis*-$[Re(bpy)_2Cl_2](PF_6)$ and its one-electron reduced form *cis*-$[Re(bpy)_2Cl_2]^0$. The structure of the former has been determined crystallographically and found to contain two neutral (bpy^0) ligands, as is indicated by the long $C_{py}-C_{py}'$ bond distance of 1.48(1) Å, and a central low-spin Re^{III} ion. The corresponding molybdenum complex *cis*-$[Mo^{III}(^{Me}bpy^0)_2Cl_2]Cl\cdot 2.5CH_3OH$ has recently been described by us.[28] Neutral *cis*-$[Re(bpy)_2Cl_2]^0$ was isolated as black crystals, but further spectroscopic characterization was not provided.[16] Given that the monocation possesses the electronic structure $[Re^{III}(bpy^0)_2Cl_2]^{1+}$ (S = 1), its one-electron reduced form can be formulated as either $[Re^{II}(bpy^0)_2Cl_2]^0$ (S = 1/2) (metal-centered reduction) or $[Re^{III}(bpy^\bullet)(bpy^0)Cl_2]^0$ (S = 1/2) (ligand-centered reduction). The black color and the associated reduction potential $E^3_{1/2}$ of −0.60 V vs Fc^+/Fc may point to the latter electronic structure. Regardless, further reduction to give the monoanionic form $[Re(bpy)_2Cl_2]^{1-}$ proceeds at a redox potential ($E^4_{1/2}$ = −1.4 V vs Fc^+/Fc) that suggests that it almost certainly proceeds via a ligand-centered reduction and yields either $[Re^{II}(bpy^\bullet)(bpy^0)Cl_2]^{1-}$ or $[Re^{III}(bpy^\bullet)_2Cl_2]^{1-}$.

The $[M(tpy)_2]^m$ (M = Mn, Tc, Re; m = 4+, 3+, 2+, 1+, 0) Series. It has been firmly established electrochemically that the series $[Mn(tpy)_2]^n$ encompasses five redox states (n = 4+ to 0),[21] and a sixth monoanionic species $[Mn(tpy)_2]^{1-}$ has been suggested to form at very negative potentials (−2.8 V vs Fc^+/Fc).[20,21] Whereas the tri- and dicationic species have been isolated and characterized by X-ray crystallography (see below), the reduced species (n < 2+) have not.

Here we report the synthesis and characterization of neutral $[Mn(tpy)_2]^0$. It was prepared by reaction of $MnBr_2$ in anhydrous THF with 2 equiv each of sodium amalgam and tpy, and upon recrystallization it was isolated as the dark green crystalline solid $[Mn(tpy)_2]^0\cdot 0.75THF$. Magnetic susceptibility measurements (4−300 K, using a SQUID magnetometer with fixed magnetic field of 1.0 T) yielded a temperature-independent magnetic moment of 3.9 μ_B (Figure 2), which is indicative of an S = 3/2 ground state. Its electronic spectrum, recorded in the range 300−1600 nm in toluene solution, plus that measured in the near IR region (2500−7000 cm^{-1}) as a the solid state sample (KBr disc), is displayed in Figure 1. In addition to the three bands observed in the UV−vis region, three additional distinct transitions are seen in the near IR (Table 2). These spectral features are similar to those observed for alkali metal salts of $(tpy^\bullet)^{1-}$[25] and are indicative of the presence of $(tpy^\bullet)^{1-}$ π-radical anions in $[Mn(tpy)_2]^0$.

From the above data and analogy to the corresponding bpy compounds, we tentatively assign the electronic structure of the neutral complex as $[Mn^{II}(tpy^\bullet)_2]^0$, where the S = 3/2 ground state of the complex is attained via antiferromagnetic coupling of the five unpaired electrons at the high-spin Mn^{II} ion with the unpaired spin of the two $(tpy^\bullet)^{1-}$ ligands. Given that the pale yellow dication is accepted to possess a $[Mn^{II}(tpy^0)_2]^{2+}$ (S = 5/2) electronic structure, assignment of the monocation as $[Mn^{II}(tpy^\bullet)(tpy^0)]^{1+}$ (S = 2) seems reasonable. By further extrapolation, the monoanionic species is most likely $[Mn^{II}(tpy^\bullet)(tpy^{\bullet\bullet})]^{1-}$ (S = 1), wherein the unpaired spins of the triplet excited state of the dianion $(tpy^{\bullet\bullet})^{2-}$ (S_L = 1) plus that of $(tpy^\bullet)^{1-}$ couple antiferromagnetically with a high-spin Mn^{II} ion to yield a triplet ground state. A similar scenario has been described for neutral $[Cr^{III}(tpy^\bullet)(tpy^{\bullet\bullet})]^0$, which possesses a singlet ground state.[3] Finally, the tetra- and tricationic species have been well characterized and are best described as $[Mn^{IV}(tpy^0)]^{4+}$ (S = 3/2) and $[Mn^{III}(tpy^0)_2]^{3+}$ (S = 2), so contain high-spin d^3 and d^4 electron configurations, respectively.[19,20] Hence, the two electron transfer processes that link these two species with the dicationic complex are firmly metal-based.

$[Tc(tpy^0)_2](BPh_4)_2\cdot H_2O$ (S = 1/2) has been isolated,[13b] but no further characterization was provided. Harmann et al.[16] reported the synthesis and characterization of $[Re(tpy)_2]PF_6$, which they formulated as $[Re^I(tpy^0)_2]^{1+}$. The accompanying electrochemical data[16] also suggests that in addition to the monocation, stable tricationic, dicationic, and neutral $[Re(tpy)_2]^m$ (m = 3+, 2+, 1+, 0) species are accessible. Indeed, the neutral complex has been synthesized and isolated.[17] Contrary to the electronic structure assignment provided by the original authors, the reported UV−vis spectrum of the monocation appears to be compatible only with the presence of $(tpy^\bullet)^{1-}$ ligand(s). In analogy with the manganese compounds, we propose the electronic structures $[Re^{II}(tpy^\bullet)(tpy^0)]^{1+}$ (S = 0) and $[Re^{II}(tpy^0)_2]^{2+}$ (S = 1/2) for the monocation and dication, respectively.

X-ray Structure Determinations. X-ray crystal structures of the homoleptic group 7 bpy complexes $[Mn(bpy)_3](ClO_4)_2\cdot 0.5H_2O$,[7] $[Tc(bpy)_3](PF_6)$,[13b] $[Re(bpy)_3][ReO_4]_2$,[15] and $[Re(bpy)_3](PF_6)$[16] have previously been reported (Chart 1); and selected $C_{py}-C_{py}'$, C−N, and M−N bond lengths averaged across the three five-membered M(bpy) chelates in these compounds are summarized in Table 4. Herein we extend this

dx.doi.org/10.1021/ic4029854 | Inorg. Chem. 2014, 53, 2276−2287

Table 4. Selected X-ray Crystallographically Determined Average Bond Lengths (Å) in $[M(bpy)_3]^n$ (M = Mn, Tc, Re)

complex	M−N	$C_{py}-C_{py}'$	C−N	T (K)[a]	ref
$[Mn^{II}(bpy^0)_3](ClO_4)_2\cdot 0.5H_2O$	2.245(5)	1.491(7)	1.343(7)	295	7
$[Li(THF)_4][Mn^{II}(bpy^{\bullet})_3]$	2.281(1)	1.425(2)	1.381(2)	100	this work
$[Mn^{II}(^{Me}bpy^{\bullet})_2(^{Me}bpy^0)]^0$	2.230(3)	1.450(5)	1.372(4)	100	this work
$[Tc^{II}(bpy^0)_3](PF_6)_2$	2.08(1)	1.48(2)	1.35(1)	*b*	13b
$[Re^{II}(bpy^0)_3](ReO_4)_2$	2.094(8)	1.482(2)	1.36(1)	295	15
$[Re^{II}(bpy^{\bullet})(bpy^0)_2](PF_6)$	2.06(1)	1.42(2)	1.39(2)	180	16

[a]Temperature of data collection. [b]Not provided.

series by determination of the structures of $[Li(THF)_4][Mn(bpy)_3]$ and $[Mn(^{Me}bpy)_3]^0$ (Figure 3). Importantly, whereas X-ray structures recorded at room temperature possess bond lengths with relatively large estimated standard deviations (esd ~0.01 or 0.02 Å), for the structure of $[Li(THF)_4][Mn(bpy)_3]$ determined at cryogenic temperatures of 100(2) K this value (~0.002 Å) is much smaller (Table 4).

In a recent paper,[28] we demonstrated that the average ligand oxidation level in $[M(bpy)_3]^m$ complexes can be determined experimentally using the *average* $C_{py}-C_{py}'$ or C−N distances of the M(bpy) chelates because they vary linearly with p in $\{(bpy)_3\}^p$. This trend originates from the fact that the same correlation between charge and $C_{py}-C_{py}'$ or C−N bond lengths exists in uncoordinated (bpy^0) and alkali metal salts of $(bpy^{\bullet})^{1-}$ and $(bpy^{2-})^{2-}$.[29] More specifically, successively filling the LUMO of (bpy^0) with one electron and then a second elicits a concomitant contraction of the $C_{py}-C_{py}'$ bond from ~1.48 to 1.43 and then 1.36 Å, and conversely elongation of the intrachelate C−N bonds from ~1.35 to 1.39 and then 1.43 Å. Hence, the *average* $C_{py}-C_{py}'$ or C−N distances in $\{(bpy)_3\}^p$-containing compounds are simply the arithmetic mean of their constituent ligands. In other words, a compound for which p = 0 contains three neutral (bpy^0) ligands, a complex possesses three $(bpy^{\bullet})^{1-}$ π-radical anions when p = 3−, and p = 6− indicates a complex with three $(bpy^{2-})^{2-}$ dianions. The intermediate cases with p = 1− and 2− correspond to complexes containing radical anions (one and two, respectively) and neutral ligands, and those with p = 4− and 5− contain dianions (one and two, respectively) and π-radical anions.

Based on the aforementioned arguments, it can be seen that the long average $C_{py}-C_{py}'$ bond lengths of 1.491(7) Å and the short average C−N distance of 1.343(7) Å in the dication $[Mn^{II}(bpy^0)_3]^{2+}$[7] are consistent with the presence of three neutral (bpy^0) ligands. This renders the oxidation state of the central manganese ion +II (d^5), and the *long* average Mn−N bond of 2.243(5) Å indicates that it is high-spin (S = 5/2).

The X-ray structure of $[Li(THF)_4][Mn(bpy)_3]$, recorded at 100 K, is well resolved with $\sigma \approx 0.002$ Å for the C−C and C−N distances. The M(bpy) chelates therein are equivalent (C_2-symmetric), and the long average Mn−N distance of 2.239 Å is comparable to that in the dication above, which is consistent with the central ion retaining a high-spin Mn^{II} state. Most saliently, the structural parameters of the *N,N′*-coordinated bpy ligands in the monoanion $[Mn^{II}(bpy)_3]^{1-}$ differ significantly from those of $[Mn^{II}(bpy^0)_3]^{2+}$, with C−C and C−N bond lengths that closely resemble those determined experimentally for the $(bpy^{\bullet})^{1-}$ anion in the salt $K(en)(bpy^{\bullet})$.[29b] The large difference in the average $C_{py}-C_{py}'$ bond lengths between the dication and anion (1.491 and 1.424 Å, respectively) of 0.067 Å is well within the resolution of the experiment, and it can be irrefutably concluded that the monoanion contains three $(bpy^{\bullet})^{1-}$ anions, which leads to assignment of its electronic structure as $[Mn^{II}(bpy^{\bullet})_3]^{1-}$.

The structure of the neutral complex $[Mn(^{Me}bpy)_3]^0$ contains two crystallographically independent molecules per unit cell. Their geometric features are identical, within 3σ, and we will, therefore, subsequently discuss only the data for molecule 1. Remarkably, the three M(^{Me}bpy) chelate rings are not identical (see Table 5), with one containing a neutral ($^{Me}bpy^0$) ligand exhibiting a characteristically long $C_{py}-C_{py}'$ distance of 1.501(5) Å and two short C−N bond lengths of 1.352(5) and 1.341(4) Å, and the other two displaying bond lengths typical of $(^{Me}bpy^{\bullet})^{1-}$ π-radical anions.[29b,c] All six Mn−N bond lengths are >2.15 Å, which is typical of a high-spin Mn^{II} ion, and whereas the average length of the four Mn−N bonds in the two Mn(^{Me}bpy$^{\bullet}$) chelates are 2.191(3) Å, the two Mn−N bonds in the Mn(^{Me}bpy^0) chelate ring are very long at 2.319(3) and 2.314(3) Å. This is primarily an electrostatic effect, with the neutral (bpy^0) ligand binding more weakly to the positively charged central metal ion than a $(^{Me}bpy^{\bullet})^{1-}$ π-radical anion. Thus, the electronic structure of the neutral complex is best described as $[Mn^{II}(^{Me}bpy^0)(^{Me}bpy^{\bullet})_2]^0$, where the S = 3/2 ground state arises from antiferromagetic coupling of the five unpaired electrons of the high-spin Mn^{II} ion with unpaired spins of the two $(bpy^{\bullet})^{1-}$ π-radicals. This electronic structure was previously forwarded by Inoue et al.[10] based solely upon magnetochemical data but has now been structurally confirmed.

Following the same rationale published structures of the dications $[Tc(bpy)_3]^{2+}$ and $[Re(bpy)_3]^{2+}$ can be analyzed.[13b,16] Both contain three neutral (bpy^0) ligands and a central low-spin divalent metal ion (Table 4), which leads to formulation of their electronic structures as $[Tc^{II}(bpy^0)_3]^{2+}$ and $[Re^{II}(bpy^0)_3]^{2+}$. This corroborates the assignments previously forwarded by the authors of the publications in which these compounds were originally described.[13,15,16]

The crystal structure of $[Re(bpy)_3](PF_6)$, which is of relatively poor quality, is worthy of comment. The original authors[16] assigned the reversible one-electron reduction of the dication $[Re^{II}(bpy^0)_3]^{2+}$ as being a metal-centered process, thereby yielding $[Re^{I}(bpy^0)_3]^{1+}$ containing three neutral (bpy^0) ligands and a low-spin Re^{I} ion (S = 0). Within the 3σ limits, quite substantial differences are observed between the C−C and C−N bond distances in the dication and monocation and have been interpreted as a π-back bonding effect from a filled t_{2g}^6 level into the LUMO of the neutral (bpy^0). However, as we[2−4] and Goicoechea et al.[5,30] have recently shown, neutral (bpy^0) is a very weak π-acceptor and does not show observable structural differences between electron poor and being bonded to electron rich metal ions. The same holds true for the *N,N′*-coordinated π-radical anion $(bpy^{\bullet})^{1-}$. Strictly speaking, the present crystal structure[16] does not allow an unambiguous assignment of the electronic structure for the monocation, but

dx.doi.org/10.1021/ic4029854 | Inorg. Chem. 2014, 53, 2276−2287

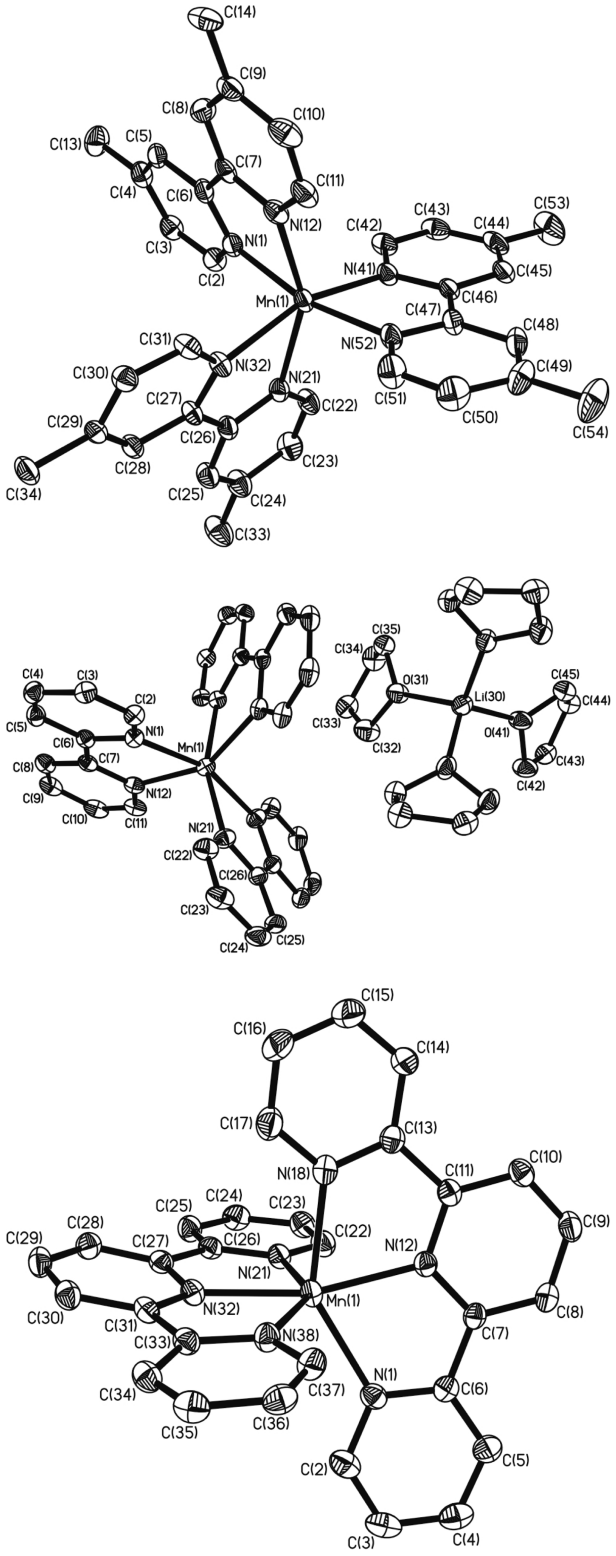

Figure 3. Structures of the complexes $[Mn^{II}(^{Me}bpy^{\bullet})_2(^{Me}bpy^0)]^0$ (top, 40% probability ellipsoids), $[Li(THF)_4][Mn^{II}(bpy^{\bullet})_3]$ (middle, 50% probability ellipsoids), and $[Mn^{II}(tpy^{\bullet})_2]^0$ (bottom, 40% probability ellipsoids). Hydrogen atoms have been omitted for clarity, and only one of two crystallographically independent molecules is shown for the neutral species.

it seems unlikely the sum charge (p) of $\{(bpy)_3\}^p$ in the monocation $[Re(bpy)_3]^+$ is zero (i.e., three neutral (bpy^0) ligands). Instead, $p = 1-$ corresponding to the electronic structure $[Re^{II}(bpy^{\bullet})(bpy^0)_2]^{1+}$ seems more probable.

Table 5. Selected Bond Distances (Å) from the Crystal Structures of $[Mn(bpy)_3]^{1-}$ and $[Mn(^{Me}bpy)_3]^0$

	$[Mn(bpy)_3]^{1-}$		
Mn−N(12)	2.230(1)	C(8)−C(9)	1.365(2)
Mn−N(21)	2.236(1)	C(9)−C(10)	1.408(2)
Mn−N(1)	2.252(1)	C(10)−C(11)	1.374(2)
N(1)−C(2)	1.349(2)	C(11)−N(12)	1.350(2)
N(1)−C(6)	1.381(2)	N(21)−C(22)	1.351(2)
C(2)−C(3)	1.374(2)	N(21)−C(26)	1.383(2)
C(3)−C(4)	1.412(2)	C(22)−C(23)	1.376(2)
C(4)−C(5)	1.365(2)	C(23)−C(24)	1.407(2)
C(5)−C(6)	1.420(2)	C(24)−C(25)	1.362(3)
C(6)−C(7)	1.427(2)	C(25)−C(26)	1.421(2)
C(7)−N(12)	1.378(2)	C(26)−C(26)′	1.422(3)
C(7)−C(8)	1.425(2)		
	$[Mn(^{Me}bpy)_3]^{0a}$		
Mn−N(52)	2.177(3)	C(6)−C(7)	1.434(5)
Mn−N(41)	2.182(3)	C(7)−N(12)	1.383(4)
Mn−N(1)	2.192(3)	C(11)−N(12)	1.339(5)
Mn−N(12)	2.213(3)	N(21)−C(22)	1.346(5)
Mn−N(32)	2.314(3)	N(21)−C(26)	1.352(5)
Mn−N(21)	2.319(3)	C(26)−C(27)	1.501(5)
N(1)−C(2)	1.347(5)	C(27)−N(32)	1.341(4)
N(1)−C(6)	1.379(5)	C(47)−N(52)	1.376(5)
C(31)−N(32)	1.339(5)	C(51)−N(52)	1.354(5)
N(41)−C(42)	1.352(4)		
N(41)−C(46)	1.387(4)		
C(46)−C(47)	1.432(5)		

[a]Data are given for ordered molecule 1.

The crystal structure of neutral $[Mn(tpy)_2]^0 \cdot 0.75THF$ presented here is of good quality, so it can be freely compared with that of $[Mn^{II}(tpy^0)_2]I_2 \cdot 3H_2O$,[18a] which is of excellent quality. All six Mn−N distances in the latter are longer than 2.20 Å; hence the Mn ion can be unequivocally assigned as possessing a +II (high-spin d^5) oxidation state. As observed for all structurally characterized M(tpy) chelates, the Mn−N distance to the central pyridine ring is significantly shorter than those to the two terminal pyridine rings (in this case $\{(Mn-N_t) - (Mn-N_c)\} \approx 0.044$ Å). Furthermore, the average $C_{py}-C_{py}'$ distance of 1.482 Å clearly indicates that, consistent with the anticipated $[Mn^{II}(tpy^0)_2]^{2+}$ ($S = 5/2$) electronic structure, both tpy ligands are neutral. Similar results have been reported for $[Mn^{III}(tpy^0)_2]^{3+}$ ($S = 2$),[19] for which the average $C_{py}-C_{py}'$ distance of 1.474 Å is also indicative of the presence of two neutral (tpy^0) ligands.

The crystal structure of the *neutral* species $[Mn(tpy)_2]^0$ (Figure 3) contains two crystallographically independent neutral molecules per monoclinic unit cell, one of which (molecule 1) is fully ordered. The other (molecule 2) displays some static disorder, which manifests as thermal parameters approximately 40% larger than those in "molecule 1". For example, carbon atom C(54) in molecule 2 has an U(eq) value of 50(1), whereas the value for the same atom C(14) in molecule 1 is only 35(1). Once again, the six Mn−N distances in molecule 1 are all >2.10 Å (Table 6), consistent with the presence of a high-spin ($S = 5/2$) Mn^{II} ion, and the two Mn−N bonds to the two central pyridine rings are significantly shorter than the four to the terminal pyridine rings. The most novel feature of this structure is the observation that for both tpy

dx.doi.org/10.1021/ic4029854 | Inorg. Chem. 2014, 53, 2276−2287

Table 6. Selected Bond Distances (Å) in the Neutral Complex $[Mn(tpy)_2]^0 \cdot 0.75THF$[a]

Mn−N(12)	2.148(2)	N(21)−C(26)	1.357(3)
Mn−N(32)	2.151(2)	C(26)−C(27)	1.468(3)
Mn−N(38)	2.238(2)	C(27)−N(32)	1.366(3)
Mn−N(1)	2.251(2)	C(31)−C(33)	1.431(4)
Mn−N(18)	2.291(2)	C(33)−N(38)	1.371(3)
Mn−N(21)	2.300(2)	C(31)−N(32)	1.384(3)
N(1)−C(6)	1.365(3)		
C(6)−C(7)	1.443(3)		
C(7)−N(12)	1.376(3)		
C(11)−N(12)	1.368(3)		
C(11)−C(13)	1.472(3)		
C(13)−N(18)	1.353(3)		

[a]Only data for molecule 1 is provided.

ligands the two five-membered chelate rings formed upon their coordination are *not* equivalent. Instead, in each tpy ligand one $C_{py}-C_{py}'$ bond is significantly shorter than the other (1.436 Å vs 1.470 Å) and can be envisaged as being a $(bpy^{\bullet})^{1-}$ π-radical anion with a fully aromatic pyridine ring attached at the 6′ position. In molecule 2, the $C_{py}-C_{py}'$ bonds in the two tpy ligands do not significantly differ from one another in length, which is a consequence of static disorder (resolution of the ligand bond lengths is insufficient for tpy asymmetry, of the type seen in molecule 1, to be discerned), but the average distance of 1.448 Å is effectively the same as that in molecule 1 (average 1.453 Å). The asymmetry observed in the tpy ligands of molecule 1 also manifests in a significant difference between the length of the Mn−N bonds to the terminal pyridine rings, with them being an average of 2.244 and 2.295 Å long. The overall average of 2.270 Å for these four bonds in molecule 1 closely matches the corresponding value of 2.239 Å in molecule 2. Not only that, but the average of all six Mn−N bond distances in molecule 1 of 2.230 Å is also very similar to the corresponding value of 2.200 Å in molecule 2. In summary, the electronic structure of the neutral species is best described as $[Mn^{II}(tpy^{\bullet})_2]^0$ with the experimentally observed $S = 3/2$ ground state (Figure 2) resulting from antiferromagnetic coupling of a high-spin Mn^{II} ion with two $(tpy^{\bullet})^{1-}$ π-radical anions.

As shown by us previously,[28] the average $C_{py}-C_{py}'$ bond length in $[Cr^{III}(tpy)_2]^{3+,2+,1+,0}$ (Figure 4), $[Mo^{IV}(tpy^{2-})_2]^0$, and $[W^{V}(tpy^{2-})(tpy^{3-})]^0$ varies linearly with the overall charge (p) of the $\{(tpy)_2\}^p$ unit (p = 0, 1−, 2−, 3−, 4−, 5−). Pleasingly, the average $C_{py}-C_{py}'$ distances in the dication $[Mn^{II}(tpy^0)_2]^{2+}$ and the neutral species $[Mn^{II}(tpy^{\bullet})_2]^0$ (1.482 and 1.450 Å, respectively) fall on this line at p = 0 in the former case and p = 2− in the latter. This demonstrates that it is possible to experimentally determine the average oxidation state of the tpy ligands in $[M(tpy)_2]^n$ complexes, regardless of the identity of the metal, using high-quality X-ray crystallography alone.

DFT Calculations. When the above experimental data for all members of the series $[Mn(bpy)_3]^n$ (n = 2+, 1+, 0, 1−) and $[Mn(tpy)_2]^m$ (m = 4+, 3+, 2+, 1+, 0) are taken together, a picture emerges wherein consecutive one-electron reductions from the dicationic starting complexes occur at localized ligand-centered orbitals to yield ligand π-radicals, which antiferromagnetically couple to a central high-spin Mn^{II} ion, thereby yielding the experimentally observed electronic ground states. To test the validity of this picture, we have undertaken a broken symmetry (BS) density functional theoretical (DFT) study of

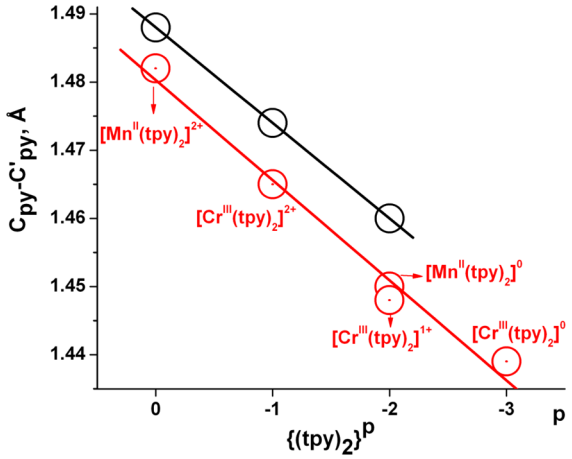

Figure 4. Experimental (red circles) and calculated (black circles) average $C_{py}-C_{py}'$ bond lengths (Å) as a function of the total charge (p) of the $\{(tpy)_2\}^p$ ligands in $[Mn^{II}(tpy)_2]^m$ and $[Cr^{III}(tpy)_2]^m$ (m = 2+, 1+, 0). The data for $[Cr(tpy)_2]^m$ is taken from ref 3, and the correlation produced using the experimental data (red line) exhibits an $R^2 = 0.991$.

these compounds at the B3LYP level of theory (see Experimental Section for further details). Where possible, the accuracy of our computational results was gauged by comparing calculated intrachelate bond lengths from geometry optimized structures with those obtained by X-ray crystallography. Good agreement between theory and experiment was, in general, obtained using the broken symmetry formalism to approximate the true multiconfigurational electronic structures of the neutral and monoanionic species. This single determinant approximation for the calculation of di- and triradicals was originally developed by Noodleman for calculating antiferromagnetically coupled di- and polymetallic clusters (i.e., metal−metal diradicals).[31] However, this approach has also been successfully applied by a number of other groups to describe metal−ligand and ligand−ligand diradicals. Calculation of spin-exchange coupling constants, J (Table 3), was performed using the Yamaguchi method (eq 3).[32] A detailed description of the meaning of the spin expectation values $\langle S^2 \rangle$ and the energies E_{HS}, and E_{BS} have been described in ref 32.

$$J = -\frac{E_{HS} - E_{BS}}{\langle S^2 \rangle_{HS} - \langle S^2 \rangle_{BS}} \quad (3)$$

The unrestricted Kohn−Sham (UKS) optimized geometry of the dication $[Mn^{II}(bpy^0)_3]^{2+}$ (S = 5/2) displays excellent agreement with experiment, with both the calculated and experimental $C_{py}-C_{py}'$ distances being 1.485 ± 0.006 Å and the corresponding average intrachelate C−N bond lengths being 1.35 ± 0.01 Å. These structural parameters closely resemble those reported for uncoordinated (bpy^0) and indicate that three neutral ligands are present in the complex.[29a] As is typically observed for B3LYP functional, the calculated M−N distances are slightly overestimated, in this case by approximately 0.05 Å. Regardless, the long Mn−N distances, both experimental and calculated, are emblematic of a high-spin d^5 electron configuration at Mn. These conclusions are corroborated by the calculated Mulliken spin density distribution (Figure 5), which places five unpaired electrons on the Mn^{II} center and negligible spin density on the bpy ligands, thereby confirming that the correct $[Mn^{II}(bpy^0)_3]^{2+}$ (S = 5/2) electronic structure was obtained.

dx.doi.org/10.1021/ic4029854 | Inorg. Chem. 2014, 53, 2276−2287

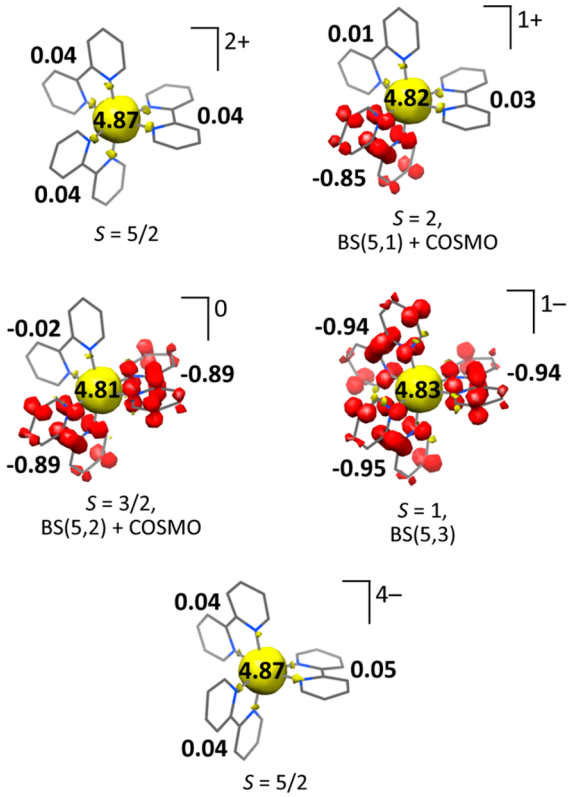

Figure 5. Calculated Mulliken spin density plots (yellow, α-spin; red, β-spin), plus spin density populations, for $[Mn(bpy)_3]^m$ (m = 2+, 1+, 0, 1−, 4−).

Geometry optimization for the monocation $[Mn^{II}(bpy^0)_2(bpy^{\bullet})]^{1+}$ (S = 2), using the UKS formalism and including a conductor like screening model (COSMO)[33] for water, yielded a BS(5,1) solution containing two neutral (bpy^0) ligands ($C_{py}-C_{py}'$ = 1.485 Å) and a single charge localized $(bpy^{\bullet})^{1-}$ π-radical anion ($C_{py}-C_{py}'$ = 1.435 Å). This charge localization was also reflected in the Mn−N bonds with those to the $(bpy^{\bullet})^{1-}$ ligand being significant shorter than those to the neutral ligands (average values of 2.198 and 2.332 Å, respectively), but both sets being long and characteristic of a central high-spin Mn^{II} ion. Interestingly, performing an analogous calculation without COSMO yielded a structure with the same average $C_{py}-C_{py}'$, C−N, and Mn−N bond distances but with a lesser degree of localization of the ligand-centered electron (Figure S1, Supporting Information). These structural parameters indicate that the electronic structure of the monocation is, as we suggested earlier, composed of two (bpy^0) ligands and one localized $(bpy^{\bullet})^{1-}$ π-radical anion, whose unpaired spin antiferromagnetically couples to a high-spin Mn^{II} ion. The Mulliken spin density analysis (Figure 5), qualitative frontier molecular orbital (FMO) diagram (Figure S11, Supporting Information), and relatively large Yamaguchi antiferromagnetic coupling constant, J_{calcd} ,of −194 cm^{-1} calculated using the localized geometry optimized structure are congruent with this idea. It should be reiterated that to date the monocation has yet to be isolated or spectroscopically characterized, so our calculated $[Mn^{II}(bpy^0)_2(bpy^{\bullet})]^{1+}$ (S = 2) ground state is in need of experimental verification.

Geometry optimization for $[Mn^{II}(bpy^{\bullet})_2(bpy)]^0$ (S = 3/2) using the UKS and BS(5,2) formalisms afforded two distinct solutions, with the former containing a low-spin Mn^{II} center and two $(bpy^{\bullet})^{1-}$ π-radical anions and being 24 kcal mol^{-1} higher in energy than the latter. In contrast, the BS(5,2) energetic ground state structure was found to possess a long average Mn−N distance of 2.275 Å, characteristic of high-spin Mn^{II}, and three equivalent bpy ligands with a relatively short average $C_{py}-C_{py}'$ distance of 1.450 Å, which is the arithmetic mean of those for two $(bpy^{\bullet})^{1-}$ anions and one (bpy^0) ligand. Inclusion of the COSMO model for water caused localization of the ligand-centered charge, yielding two $(bpy^{\bullet})^{1-}$ ligands with an average $C_{py}-C_{py}'$ distance of 1.433 Å and a single neutral ligand with a $C_{py}-C_{py}'$ bond length of 1.484 Å. This is reflected in the corresponding spin density plot and FMO diagram (Figure 5 and Figure S12, Supporting Information, respectively), both of which place five unpaired electrons of α-spin on the Mn ion and two electrons of β-spin on the ligands, one on each of two of the bpy ligands. The experimentally observed S = 3/2 ground state is then attained via antiferromagnetic coupling of the metal- and ligand-centered spins, for which a J_{calcd} of −156 cm^{-1} was calculated. This is in excellent agreement with the experimental value of −140 cm^{-1} (Table 3).

Similarly, a UKS calculation for $[Mn^{II}(bpy^{\bullet})_3]^{1-}$ (S = 1) provided a geometry optimized structure containing a low-spin Mn^{II} ion and three $(bpy^{\bullet})^{1-}$ ligands (Figure S4, Supporting Information), but it was found to be 26 kcal mol^{-1} higher in energy than the BS(5,3) solution. The structural parameters of the BS(5,3) ground state display excellent agreement with the X-ray structure of the monoanion detailed above. For example, the average calculated and experimental intrachelate C−N bond lengths of 1.385 and 1.381 Å, respectively; and the long average calculated Mn−N distance of 2.275 Å nicely reproduces the corresponding experimental value of 2.239 Å. Furthermore, the average calculated $C_{py}-C_{py}'$ bond length of 1.433 Å is very similar to the value of 1.431(3) Å found in the $(bpy^{\bullet})^{1-}$ π-radical anion in the X-ray structure of K(en)($bpy^{\bullet}$). These structural parameters are all consistent with the previously forwarded formulation $[Mn^{II}(bpy^{\bullet})_3]^{1-}$, wherein three equivalent π-radical $(bpy^{\bullet})^{1-}$ ligands antiferromagnetically couple with the high-spin Mn^{II} center to produce the observed S = 1 ground state. The qualitative FMO diagram (Figure S13, Supporting Information) and spin density plot (Figure 5) confirm this scenario, and the accompanying antiferromagnetic coupling constant of −100 cm^{-1} is in excellent agreement with experiment (Table 3), thereby validating the quality of the calculations.

Finally, UKS geometry optimization of $[Mn^{II}(bpy^{2-})_3]^{4-}$ (S = 5/2) converged to a structure containing three equivalent bpy ligands possessing a very short average $C_{py}-C_{py}'$ distance of 1.381 Å and a very long average intrachelate C−N bond length of 1.426 Å, which are typical of diamagnetic $(bpy^{2-})^{2-}$ ligands. Combined with the long average Mn−N distance of 2.356 Å, which is consistent with retention of a high-spin Mn^{II} center, it is clear that the electronic structure description $[Mn^{II}(bpy^{2-})_3]^{4-}$ is most appropriate. Consistent with this notion, a Mulliken spin density analysis (Figure 5) places 4.9 unpaired spins on the metal ion and virtually no spin density on the ligands, and the qualitative FMO diagram (Figure S14, Supporting Information) contains three doubly occupied bpy π^*-orbitals.

Figure 6 shows the experimentally determined and calculated average $C_{py}-C_{py}'$ bond lengths in $[Mn^{II}(bpy)_3]^n$ (n = 2+, 1+, 0, 1−, 4−) as a function of the total charge (p) of the three bpy ligands $\{(bpy)_3\}^p$, where p = 0 corresponds to three neutral

dx.doi.org/10.1021/ic4029854 | Inorg. Chem. 2014, 53, 2276−2287

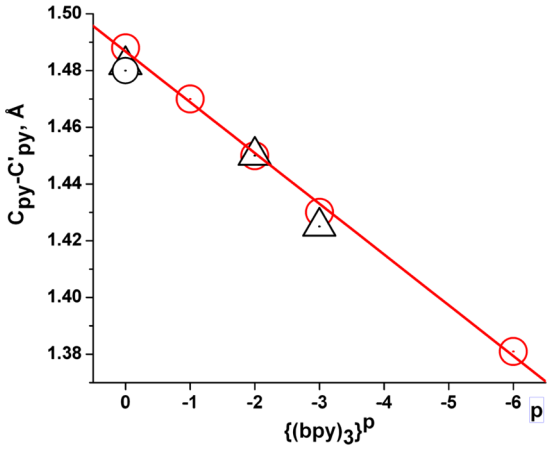

Figure 6. Experimental (black triangles) and calculated (red circles) average $C_{py}-C_{py}'$ bond lengths (Å) as a function of the total charge (p) of the $\{(bpy)_3\}^p$ ligands in $[Mn(bpy)_3]^m$ (m = 2+, 1+, 0, 1−, 4−). The correlation produced using the calculated data (red line) exhibits an R^2 = 0.993. The black circle represents the corresponding experimental values for $[M(bpy)_3]^{2+}$, where M = Tc[13b] and Re.[15]

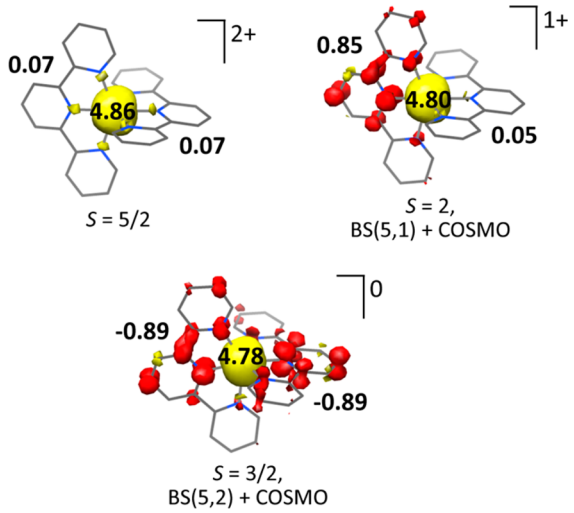

Figure 7. Calculated Mulliken spin density plots (yellow, α-spin; red, β-spin), plus spin density populations, for $[Mn(tpy)_2]^m$ (m = 2+, 1+, 0).

(bpy^0) ligands, p = 1− to one $(bpy^{\bullet})^{1-}$ and two (bpy^0), p = 2− to two $(bpy^{\bullet})^{1-}$ and one (bpy^0), p = 3− to three $(bpy^{\bullet})^{1-}$, and p = 6− to three diamagnetic $(bpy^{2-})^{2-}$ dianions. As previously demonstrated for other $[M(bpy)_3]^n$ complexes, the calculated average $C_{py}-C_{py}'$ distance varies linearly with p (red line). Gratifyingly, the arithmetic mean of the experimental $C_{py}-C_{py}'$ distances for dicationic (p = 0) $[Mn^{II}(bpy^0)_3]^{2+}$,[7] $[Tc^{II}(bpy^0)_3]^{2+}$,[13] and $[Re^{II}(bpy^0)_3]^{2+}$,[16] the neutral complex $[Mn^{II}(^{Me}bpy^{\bullet})_2(^{Me}bpy^0)]^0$ (p = 2−), and the monoanion $[Mn^{II}(bpy^{\bullet})_3]^{1-}$ (p = 3−) all fall on this line. This is strong evidence to support the notion that the sum charge p of the three coordinated bpy ligands, from which their individual oxidation states can be extrapolated, can be determined experimentally by high-resolution X-ray crystallography.

Using the computational methodology described above for the $[Mn^{II}(bpy)_3]^n$ series, we have also calculated the optimized geometries and electronic structures of the three complexes $[Mn^{II}(tpy)_3]^m$ (m = 2+, 1+, 0). Calculations for the dication $[Mn^{II}(tpy^0)_2]^{2+}$ (S = 5/2) converged to a structure displaying excellent agreement with experiment,[18] containing two neutral C_2-symmetrically N,N',N''-coordinated (tpy^0) ligands bound to a high-spin Mn^{II} ion. This is reflected in the calculated Mulliken spin density plot, shown in Figure 7, which carries effectively zero spin density on the (tpy^0) ligands and five unpaired electrons at the Mn center.

UKS calculations of the corresponding monocation, carried out with the inclusion of COSMO for water, yield a optimized geometry possessing a charge localized structure containing one neutral (tpy^0) ligand and one $(tpy^{\bullet})^{1-}$ π-radical anion coordinated to a high-spin Mn^{II} ion. This is evident in their respective average $C_{py}-C_{py}'$ distances of 1.466 Å for $(tpy^{\bullet})^{1-}$ and 1.487 Å for (tpy^0), which are clearly different, and the fact that all the Mn−N distances are long (>2.19 Å). Thus, the electronic structure of this complex is best described as $[Mn^{II}(tpy^{\bullet})(tpy^0)]^{1+}$, wherein the unpaired electrons of the high-spin Mn^{II} center couple antiferromagnetically to a ligand-centered spin on the π-radical anion (J_{calcd} = −200 cm^{-1}) to yield an S = 2 ground state. The calculated Mulliken spin density plot and qualitative FMO diagram (Figure 7 and Figure S16, Supporting Information, respectively) corroborate this assertion. This electronic structure description is in stark contrast to that of the analogous monocationic complex $[Mn^{III}(pdi^{\bullet})_2]^{1+}$ (S = 0; pdi = 2,6-bis[1-(4-methoxyphenylimino)ethyl]pyridine), which contains a low-spin Mn^{III} ion antiferromagnetically coupled to two ligand radicals. The difference between the electronic ground states of these two closely comparable complexes can be attributed to the greater ligand field strength of the pdi ligand relative to tpy. This is nicely illustrated by the corresponding dicationic cobalt complexes $[Co^{II}(pdi^0)_2]^{2+}$ and $[Co^{II}(tpy^0)_2]^{2+}$, where the former is low-spin (S = 1/2) at room temperature[34] and the latter is widely known to display spin-crossover below ambient temperatures.

Finally, geometry optimization of the neutral complex $[Mn^{II}(tpy^{\bullet})_2]^0$ (S = 3/2), using the BS(5,2) formalism and the COSMO for water, affords a structure in which the two tpy ligands differ. As shown in Figure 8, one $(tpy^{\bullet})^{1-}$ ligand is asymmetrically N,N',N''-coordinated and has two different $C_{py}-C_{py}'$ bond lengths of 1.467 and 1.453 Å, whereas the other N,N',N''-coordinated $(tpy^{\bullet})^{1-}$ ligand is C_2-symmetric and has two equal $C_{py}-C_{py}'$ distances of 1.46 Å. However, in both ligands, the average $C_{py}-C_{py}'$ distance is the same (i.e., 1.46 Å), which indicates that both ligands possess the same oxidation level, namely, that of a $(tpy^{\bullet})^{1-}$ π-radical anion. Once again, all Mn−N bonds are long (>2.17 Å) and indicate that a high-spin Mn^{II} ion is present. Taken as a whole, the calculated geometry is in excellent agreement with experiment (Figure 8), with the specific structural parameters of the asymmetrically coordinated Mn(tpy) chelate ring closely resembling those of molecule 1 in the X-ray structure (Figure 8A) and the symmetrically coordinated Mn(tpy) chelate ring resembling those of molecule 2 (Figure 8B). The Mulliken spin density plot and qualitative FMO diagram (Figure 7 and Figure S17, Supporting Information, respectively) confirm this picture with the different distribution of spin density in the two tpy ligands readily apparent.

■ CONCLUSION

The most prominent feature of this investigation is the observation that it is possible to assign the redox states of the three bpy ligands in $[Mn(bpy)_3]^n$ (n = 2+, 1+, 0, 1−, 4−) and

dx.doi.org/10.1021/ic4029854 | Inorg. Chem. 2014, 53, 2276−2287

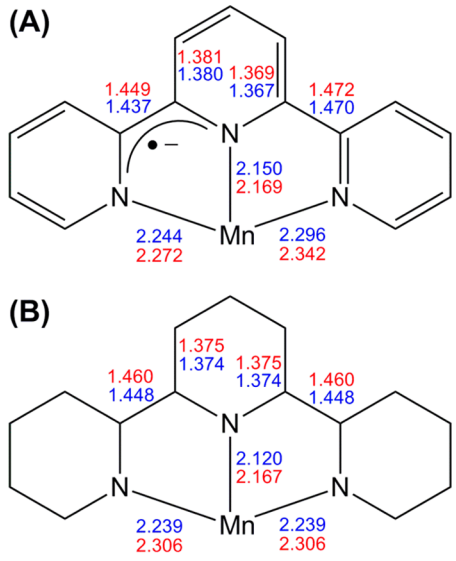

Figure 8. (A) Asymmetric coordination of $(tpy^{\bullet})^{1-}$ seen in molecule 1 of the X-ray structure of $[Mn^{II}(tpy^{\bullet})_2]^0$, and one of the ligands in the BS(5,2) DFT geometry optimized structure of this complex calculated with inclusion of COSMO for water. (B) Symmetric coordination of $(tpy^{\bullet})^{1-}$ seen in molecule 2 of the X-ray structure of $[Mn^{II}(tpy^{\bullet})_2]^0$, and the second ligand of the aforementioned DFT geometry optimized structure of this complex. Values in red are DFT calculated and those in blue are from the X-ray structure.

two tpy ligands in $[Mn(tpy)_2]^m$ (n = 3+, 2+, 1+, 0) solely using X-ray crystallographically determined intraligand structural parameters. More specifically, the arithmetic mean of the $C_{py}-C_{py}'$ distances in $\{(bpy)_3\}^p$ and $\{(tpy)_2\}^p$ decreases linearly with increasing total charge (p). Second, the Mn center in all complexes with charge $(n/m) < 2$ retain the high-spin d^5 electron configuration of the dicationic species. In other words, as previously postulated by Inoue and co-workers for the $[Mn(bpy)_3]^n$ series[10] and observed for a number of other series of $[M(bpy)_3]^n$ and $[M(tpy)_2]^m$ complexes, reduction of the dications to more negatively charged species is purely ligand-centered. Hence, the $[Mn(bpy)_3]^n$ series members possess the electronic structures $[Mn^{II}(bpy^0)_3]^{2+}$ (S = 5/2), $[Mn^{II}(bpy^{\bullet})(bpy^0)_2]^{1+}$ (S = 2), $[Mn^{II}(bpy^{\bullet})_2(bpy^0)]^0$ (S = 3/2), $[Mn^{II}(bpy^{\bullet})_3]^{1-}$ (S = 1), and $[Mn^{II}(bpy^{2-})_3]^{4-}$ (S = 5/2); and the electronic structures of the $[Mn(tpy)_2]^m$ series are $[Mn^{III}(tpy^0)_2]^{3+}$ (S = 2), $[Mn^{II}(tpy^0)_2]^{2+}$ (S = 5/2), $[Mn^{II}(tpy^{\bullet})(tpy^0)]^{1+}$ (S = 2), and $[Mn^{II}(tpy^{\bullet})_2]^0$ (S = 3/2). The electron spin ground states are determined throughout by antiferromagnetic coupling of the high-spin Mn^{II} center (S_{Mn} = 5/2) with any π-radical anions (S_L = 1/2) present.

These conclusions were fully supported by BS-DFT calculations, with the agreement between calculated and experimentally determined structural parameters and electron−electron exchange coupling constants (J) being excellent. A further point of note is that inclusion of COSMO for water in geometry optimizations for the complexes containing ligands of differing valency (i.e., the monocations and the neutral complex in the bpy series) causes charge localization. Assorted experimental evidence supports this picture, and based on the relatively large number of X-ray structures of bpy and tpy complexes of this type that we have now collected,[2,3] charge localization appears to be the norm. The structures for which charge localization was not observed are, by-and-large, poor quality structures plagued by static disorder or those belonging to a symmetry group that renders the ligands equivalent.

For the analogous Tc and Re series of complexes, the dicationic species clearly contain three neutral (bpy^0) or two neutral (tpy^0) ligands and a central low-spin $4d^5$ or $5d^5$ metal ion, but more experimental work (spectroscopy) is required before concrete assignment of the electronic structures of more reduced species (n/m < 2) will be possible. However, by comparison of the electrochemistry reported for these species with that of their Mn analogues, it seems likely that species with a charge <2+ will once again contain reduced ligands and not metal ions with an oxidation state of ≤ I+.

EXPERIMENTAL SECTION

Synthesis of Compounds. Unless stated otherwise, all syntheses were carried out in the absence of water and dioxygen, under an argon atmosphere, using standard Schlenk techniques or a glovebox. The ligands 4,4′-dimethyl-2,2′-bipyridine (^{Me}bpy), 2,2′-bipyridine (bpy), and 2,2′:6′,2″-terpyridine (tpy), the starting material $MnBr_2$, and the reductants lithium metal and 10% sodium amalgam were all purchased from commercial vendors and used without purification. The complex $[Li(THF)_4][Mn(bpy)_3]$ was prepared using a published procedure.[11]

[Mn(^{Me}bpy)$_3$]^0. A mixture of 3 equiv of ^{Me}bpy (0.55 g, 3.0 mmol), 1 equiv of $MnBr_2$ (0.21 g, 1.0 mmol), and 2 equiv of sodium amalgam (10 wt %; 0.5 g, ∼2.0 mmol) in 25 mL of THF was stirred at ambient temperature for 48 h. The resulting purple solution was filtered, and all volatiles were removed *in vacuo*. The residue obtained was dissolved in dry toluene and filtered, and the solvent was removed under reduced pressure to yield solid, which was washed with *n*-pentane and dried to give 0.14 g (22% yield) of dark purple product. Unfortunately, a satisfactory elemental analysis could not be obtained. Vapor diffusion of *n*-pentane into a saturated toluene solution of crude material obtained directly from the reaction mixture at −20 °C provided single crystals of $[Mn(^{Me}bpy)_3]^0\cdot(n\text{-pentane})\cdot 0.5THF\cdot 0.25(^{Me}bpy)$ suitable for X-ray crystallography.

[Mn(tpy)$_2$]^0. This complex was prepared using an analogous procedure to that described for $[Mn(^{Me}bpy)_3]^0$, but with 2 equiv of tpy in place of the 3 equiv of ^{Me}bpy. Yield: 0.16 g (31%). X-ray quality dark green crystals of the solvate $[Mn(tpy)_2]\cdot 0.75THF$ were grown by vapor diffusion of *n*-pentane into a saturated THF solution of complex at −20 °C. Anal. Calcd for $C_{30}H_{22}MnN_6$: C, 69.10; H, 4.25; N, 16.12. Found: C, 68.75; H, 4.12; N, 15.96.

X-ray Crystallographic Data Collection and Refinement of the Structures. Single crystals of complexes $[Mn(^{Me}bpy)_3]^0$, $[Li(thf)_4][Mn(bpy)_3]$, and $[Mn(tpy)_2]^0$ were coated with perfluoropolyether, picked up with nylon loops, and mounted in the nitrogen cold stream of the diffractometer. Graphite monochromated Mo Kα radiation (λ = 0.71073 Å) from a Mo-target rotating-anode X-ray source was used throughout. Final cell constants were obtained from least-squares fits of several thousand strong reflections. Intensity data were corrected for absorption using intensities of redundant reflections with the program SADABS.[35] The structures were readily solved by Patterson methods and difference Fourier techniques. The Siemens ShelXTL[36] software package was used for solution, refinement, and rendering of the structures. All non-hydrogen atoms were anisotropically refined, and hydrogen atoms were placed at calculated positions and refined as riding atoms with isotropic displacement parameters.

The unit cell of $[Mn(^{Me}bpy)_3]^0$ contains eight neutral complex molecules and at least four pentane, four tetrahydrofuran (THF), and two bipyridyl (bpy) molecules. A similar situation applies for $[Mn(tpy)_2]^0$, which contains eight neutral complex molecules and six THF molecules per unit cell. Both structures, including solvent molecules, were fully refined. However, the solvent molecules were found to be severely disordered and could not be satisfactorily refined by split atom models, so a Platon-Squeeze[37] was used to refine the solvent-free structures. Crystallographic data of the compounds are listed in Table 7.

dx.doi.org/10.1021/ic4029854 | Inorg. Chem. 2014, 53, 2276−2287

Table 7. Crystallographic Data of Complexes

	$[Mn(^{Me}bpy)_3]$	$[Li(THF)_4][Mn(bpy)_3]$	$[Mn(tpy)_2]$
chem. formula	$C_{36}H_{36}MnN_6$	$C_{46}H_{56}LiMnN_6O_4$	$C_{30}H_{22}MnN_6$
FW	607.65	818.84	648.65
space group	$P2_1/n$, No. 14	*Pbcn*, No. 60	$P2_1/c$, No. 14
a, Å	19.400(3)	12.841(3)	16.321(4)
b, Å	14.171(2)	17.827(4)	18.167(4)
c, Å	30.796(4)	18.182(4)	18.187(4)
β, deg	94.807(3)	90	95.479(4)
V, Å	8437(2)	4162(2)	5368(2)
Z	8	4	8
T, K	100(2)	100(2)	100(2)
ρ calcd, g cm^{-3}	0.957[d]	1.307	1.291[d]
reflns collected/ $2\Theta_{max}$	107225/52.04	103534/62.15	113559/53.61
unique reflns/$I > 2\sigma(I)$	16613/10815	6664/4851	11407/7402
no. of params/ restraints	787/0	276/11	668/0
λ, Å/μ(Kα), cm^{-1}	0.71073/3.39[d]	0.71073/3.68	0.71073/5.21[d]
R1[a]/GOF[b]	0.0693/1.038	0.0409/1.028	0.0427/1.021
wR2[c] ($I > 2\sigma(I)$)	0.1594	0.0906	0.0905
residual density, e Å^{-3}	+0.55/−0.73	+0.57/−0.30	+0.43/−0.55

[a]Observation criterion: $I > 2\sigma(I)$. R1 = $\sum||F_o| - |F_c||/\sum|F_o|$. [b]GOF = $[\sum[w(F_o^2 - F_c^2)^2]/(n - p)]^{1/2}$. [c]wR2 = $[\sum[w(F_o^2 - F_c^2)^2]/\sum[w(F_o^2)^2]]^{1/2}$, where $w = 1/\sigma^2(F_o^2) + (aP)^2 + bP$, $P = (F_o^2 + 2F_c^2)/3$. [d]Data given for the solvent-free crystal.

Calculations. All DFT calculations were performed using version 3.0 of the ORCA software package.[38] The geometries of all complexes were optimized in redundant internal coordinates without imposing geometry constraints, and all subsequent single point calculations were performed at the B3LYP level of theory.[39] In all calculations, the TZVP basis set was applied to all atoms.[40] Auxiliary basis sets, used to expand the electron density in the calculations, were chosen to match the orbital basis sets.[41] The RIJCOSX approximation was used to accelerate the calculations.[42]

The self-consistent field calculations were tightly converged (1×10^{-8} E_h in energy, 1×10^{-7} E_h in the density charge, and 1×10^{-7} in the maximum element of the DIIS[43] error vector). In all cases, the geometries were considered converged after the energy change was less than 1×10^{-6} E_h, the gradient norm and maximum gradient element were smaller than 3×10^{-5} and 1×10^{-4} E_h bohr^{-1}, respectively, and the root-mean-square and maximum displacements of all atoms were smaller than 6×10^{-4} and 1×10^{-3} bohr, respectively. The authenticity of each converged structure was confirmed by the absence of imaginary vibrational frequencies.

Interestingly, performing identical calculations using the more diffuse def2-TZVP basis set[44] resulted in incorrect electronic structures and manifested as a large disparity between the calculated and experimental structural parameters. For example, geometry optimization for $S = 5/2$ $[Mn(bpy)_3]^{2+}$, which is known to contain high-spin Mn^{II} and three neutral (bpy^0) ligands and to exhibit average Mn−N distances of approximately 2.2 Å, yielded a Mn^{IV} species containing one (bpy^0) and two $(bpy^{\bullet})^{1-}$ ligands and an average Mn−N bond length of 1.88 Å. It was found that this problem could be corrected by implementation of the zeroth-order regular approximation (ZORA) method,[45] but given that the results obtained were qualitatively identical to those using the computationally less demanding TZVP basis set, the latter was preferentially used throughout. Additionally, the gas-phase calculations for the ground states of both types of complex $[Mn(bpy)_3]^n$ and $[Mn(tpy)_2]^n$ were repeated using the conductor-like screening model (COSMO),[33] with water as the solvent. This caused charge localization and concomitant structural changes in all cases.

Throughout this study, our computational results are described using the broken symmetry (BS) approach.[31] The following notation is used to describe the BS solutions, where the given system is divided into two fragments. The notation BS(m,n) refers to an open-shell BS state with m unpaired α-spin electrons localized on fragment 1 and n unpaired β-spin electrons localized on fragment 2. In this notation, the standard high-spin, open-shell solution is written as BS($m + n$,0). The BS(m,n) notation refers to the initial guess for the wave function. The variational process does, however, have the freedom to converge to a solution of the form BS($m - n$,0), in which the $n\beta$-spin electrons effectively pair up with $n < m$ α-spin electrons on the partner fragment. Such a solution is then a standard $M_s \cong (m - n)/2$ spin-unrestricted or spin-restricted Kohn−Sham solution. As explained elsewhere,[46] the nature of the solution is investigated from corresponding orbital transformation (COT), which from the corresponding orbital overlaps displays whether the system should be described as a spin-coupled or a closed-shell solution. Orbitals and density plots were created using Chimera.[47]

■ ASSOCIATED CONTENT

Supporting Information

Crystallographic information files (cif) for the complexes $[Mn^{II}(^{Me}bpy^{\bullet})_2(^{Me}bpy^0)]^0$, $[Li(THF)_4][Mn^{II}(bpy^{\bullet})_3]$, and $[Mn^{II}(tpy^{\bullet})_2]^0$ and further information regarding the DFT calculations, including tables of atomic coordinates, bond distances, and energies, and additional Mulliken spin density plots and qualitative frontier molecular orbital diagrams. This material is available free of charge via the Internet at http://pubs.acs.org.

■ AUTHOR INFORMATION

Corresponding Author

*Email: karl.wieghardt@cec.mpg.de.

Author Contributions

‡M.W. and J. E. contributed equally.

Notes

The authors declare no competing financial interest.

■ ACKNOWLEDGMENTS

M.W. and J.E. thank the Max Planck Society for financial support and Mr. Andreas Göbels for technical assistance.

■ REFERENCES

(1) Comprehensive reviews of $[M(bpy)_3]^n$ and $[M(tpy)_2]^m$ complexes have been published: (a) Constable, E. C. *Adv. Inorg. Chem.* **1989**, *34*, 1. (b) Constable, E. C. *Adv. Inorg. Chem.* **1986**, *31*, 69.

(2) Scarborough, C. C.; Sproules, S.; Weyhermüller, T.; DeBeer, S.; Wieghardt, K. *Inorg. Chem.* **2011**, *50*, 12446 and references therein.

(3) Scarborough, C. C.; Lancaster, K. M.; DeBeer, S.; Weyhermüller, T.; Sproules, S.; Wieghardt, K. *Inorg. Chem.* **2012**, *51*, 3718.

(4) (a) Scarborough, C. C.; Wieghardt, K. *Inorg. Chem.* **2011**, *50*, 9773. (b) Bowman, A. C.; Sproules, S.; Wieghardt, K. *Inorg. Chem.* **2012**, *51*, 3707.

(5) Irwin, M.; Doyle, L. R.; Krämer, T.; Herchel, R.; McGrady, J. E.; Goicoechea, J. M. *Inorg. Chem.* **2012**, *51*, 12301.

(6) (a) Martin, B.; McWinnie, W. R.; Waind, G. M. *J. Inorg. Nucl. Chem.* **1961**, *23*, 207. (b) Burstall, F. H.; Nyholm, R. S. *J. Chem. Soc.* **1952**, 3570.

(7) Chen, X.-M.; Wang, R.-Q.; Xu, Z.-T. *Acta Crystallogr.* **1995**, *C51*, 820.

(8) (a) Clark, R. J. H.; Willis, C. S. *Spectrochim. Acta, Part A* **1967**, *23A*, 1055. (b) Morrison, M. M.; Sawyer, D. T. *Inorg. Chem.* **1978**, *17*, 333.

(9) Herzog, S.; Schmidt, M. *Z. Chem.* **1962**, *2*, 24.

(10) Inoue, M.; Hara, K.; Horiba, T.; Kubo, M. *Bull. Chem. Soc. Jpn.* **1974**, *47*, 2137.

(11) Herzog, S.; Schmidt, M. *Z. Chem.* **1963**, *3*, 392.
(12) (a) Herzog, S.; Grimm, U. *Z. Chem.* **1967**, *7*, 432. (b) Kaizu, Y.; Yazaki, T.; Torii, Y.; Kobayashi, H. *Bull. Chem. Soc. Jpn.* **1970**, *43*, 2068.
(13) (a) Archer, C. M.; Dilworth, J. R.; Kelby, D.; McPartlin, M. *Polyhedron* **1989**, *8*, 1879. (b) Archer, C. M.; Dilworth, J. R.; Thompson, R. M.; McPartlin, M.; Povey, D. C.; Kelly, J. D. *J. Chem. Soc., Dalton Trans.* **1993**, 461.
(14) Chakravorty, M. C.; Sen, B. K. *J. Ind. Chem. Soc.* **1966**, *43*, 464.
(15) Stebler, M.; Gutiérrez, A.; Luchi, A.; Bürgi, H.-B. *Inorg. Chem.* **1987**, *26*, 1449.
(16) Helberg, L. F.; Orth, S. D.; Sabath, M.; Harman, W. D. *Inorg. Chem.* **1996**, *35*, 5584.
(17) Quirk, J.; Wilkinson, G. *Polyhedron* **1982**, *1*, 209.
(18) (a) Baffert, C.; Romero, I.; Péccaut, J.; Llobet, A.; Deronzier, A.; Collomb, M.-N. *Inorg. Chim. Acta* **2004**, *357*, 3430. (b) Oshio, H.; Spiering, H.; Ksenofontov, V.; Renz, F.; Gütlich, P. *Inorg. Chem.* **2001**, *40*, 1143. (c) Bhula, R.; Weatherburn, D. C. *Aust. J. Chem.* **1991**, *44*, 303. (d) Freire, E.; Baggio, S.; Garland, M. T.; Baggio, R. *Acta Crystallogr.* **2001**, *C57*, 1403. (e) Sjödin, M.; Gätjens, J.; Tabares, L. C.; Thuéry, P.; Pecoraro, V. L. *Inorg. Chem.* **2008**, *47*, 2897.
(19) Romain, S.; Duboc, C.; Neese, F.; Rivière, E.; Hanton, L. R.; Blackman, A. G.; Philouze, C.; Leprêtre, J.-S.; Deronzier, A.; Collomb, M.-N. *Chem.—Eur. J.* **2009**, *15*, 980.
(20) Romain, S.; Baffert, C.; Duboc, C.; Leprêtre, J.- C.; Deronzier, A.; Collomb, M.−N. *Inorg. Chem.* **2009**, *48*, 3125.
(21) (a) Sato, Y.; Tanaka, N. *Bull. Chem. Soc. Jpn.* **1968**, *41*, 2064. (b) Hughes, M. C.; Rao, J. M.; Macero, D. *Inorg. Chim. Acta* **1979**, *35*, L321. (c) Hughes, M. C.; Rao, J. M.; Macero, D. *Inorg. Chim. Acta* **1976**, *18*, 127.
(22) England, J.; Scarborough, C. C.; Weyhermüller, T.; Sproules, S.; Wieghardt, K. *Eur. J. Inorg. Chem.* **2012**, 4605. (b) Rao, J. M.; Hughes, M. C.; Macero, J. *Inorg. Chim. Acta* **1979**, *35*, L369.
(23) (a) Chsawa, Y.; DeArmond, M. K.; Hauck, K. W.; Morris, D. E. *J. Am. Chem. Soc.* **1963**, *105*, 6522. (b) Saji, T.; Aoyagui, S. *J. Electroanal. Chem.* **1975**, *58*, 401.
(24) König, E.; Kremer, S. *Chem. Phys. Lett.* **1970**, *5*, 87.
(25) Braterman, P.; Song, J.-I.; Peacock, R. D. *Inorg. Chem.* **1992**, *31*, 555.
(26) Heath, G. A.; Yellowlees, L. J.; Braterman, P. S. *J. Chem. Soc., Chem. Commun.* **1981**, 281.
(27) Kirmse, R.; Abram, U. *Z. Anorg. Allg. Chem.*. **1992**, *608*, 184.
(28) Wang, M.; Weyhermüller, T.; England, J.; Wieghardt, K. *Inorg. Chem.* **2013**, *52*, 12763.
(29) (a) Chisholm, M. M.; Huffman, J. C.; Rothwell, I. P.; Bradley, P. G.; Kress, N.; Woodruff, J. M. *J. Am. Chem. Soc.* **1981**, *103*, 4945. (b) Gore-Randall, E.; Irwin, E.; Denning, M. S.; Goicoechea, J. M. *Inorg. Chem.* **2009**, *48*, 8304. (c) Echegoyen, L.; DeCiam, A.; Fischer, J.; Lehn, J.-M. *Angew. Chem., Int. Ed.* **1991**, *30*, 838. (d) Bock, H.; Lehn, J.-M.; Pauls, J.; Holl, S.; Krenzel, V. *Angew. Chem., Int. Ed.* **1999**, *38*, 952.
(30) Irwin, M.; Jenkins, R. K.; Denning, M. S.; Krämer, T.; Grandjean, F.; Long, G. J.; Herchel, R.; McGrady, J. E.; Goicoechea, J. M. *Inorg. Chem.* **2010**, *49*, 6160.
(31) (a) Noodleman, L. *J. Chem. Phys.* **1981**, *74*, 5737. (b) Noodleman, L.; Norman, J. G.; Osborne, J. H.; Aizman, A.; Case, D. *J. Am. Chem. Soc.* **1985**, *107*, 3418. (c) Noodleman, L.; Davidson, E. R. *Chem. Phys.* **1986**, *109*, 131. (d) Noodleman, L.; Case, D. A.; Aizman, A. J. *J. Am. Chem. Soc.* **1988**, *110*, 1001. (e) Noodleman, L.; Peng, C. Y.; Case, D. A.; Monesca, J. M. *Coord. Chem. Rev.* **1995**, *144*, 199.
(32) (a) Soda, T.; Kitagawa, Y.; Onishi, T.; Takano, Y.; Shigeta, Y.; Nagao, H.; Yoshioka, Y.; Yamaguchi, K. *Chem. Phys. Lett.* **2000**, *319*, 223. (b) Yamaguchi, K.; Takahara, Y.; Fueno, T. In *Applied Quantum Chemistry*; Smith, V. H., Ed.; Reidel: Dordecht, The Netherlands, 1986; p 155.
(33) Klamt, A.; Schüürmann, G. *J. Chem. Soc., Perkin Trans. 2* **1993**, 799.
(34) de Bruin, B.; Bill, E.; Bothe, E.; Weyhermüller, T.; Wieghardt, K. *Inorg. Chem.* **2000**, *39*, 2936.
(35) Sheldrick, G. M. SADABS, Bruker-Siemens Area Detector Absorption and Other Corrections, Version 2008/1, Universität Göttingen: Germany, 2006.
(36) ShelXTL 6.14, Bruker AXS Inc.: Madison, WI, USA, 2003.
(37) Platon Program Suite: Spek, A. L. *Acta Crystallogr.* **2009**, *D65*, 148.
(38) Neese, F. *WIREs Comput. Mol. Sci.* **2012**, *2*, 73. The ORCA program is available free of charge at www.cec.mpg.de/downloads.html.
(39) (a) Becke, A. D. *Phys. Rev. A* **1988**, *38*, 3098. (b) Becke, A. D. *J. Chem. Phys.* **1993**, *98*, 5648. (c) Lee, C. T.; Yang, W. T.; Parr, R .G. *Phys. Rev. B* **1988**, *37*, 785.
(40) (a) Schaefer, A.; Horn, H.; Ahlrichs, R. *J. Chem. Phys.* **1992**, *97*, 2571. (b) Schäfer, A.; Huber, C.; Ahlrichs, R. *J. Chem. Phys.* **1994**, *100*, 5829.
(41) (a) Eichkorn, K.; Weigend, F.; Treutler, O.; Ahlrichs, R. *Theor. Chem. Acc.* **1997**, *97*, 119. (b) Eichkorn, K.; Treutler, O.; Öhm, H.; Häser, M.; Ahlrichs, R. *Chem. Phys. Lett.* **1995**, *242*, 652.
(42) (a) Neese, F.; Wennmohs, F.; Hansen, A.; Becker, U. *Chem. Phys.* **2009**, *356*, 98. (b) Kossmann, S.; Neese, F. *Chem. Phys. Lett.* **2009**, *481*, 240. (c) Neese, F. *J. .Comput. Chem.* **2003**, *24*, 1714.
(43) (a) Pulay, P. *Chem. Phys. Lett.* **1980**, *73*, 393. (b) Pulay, P. *J. Comput. Chem.* **1982**, *3*, 556.
(44) Weigend, F.; Ahlrichs, R. *Phys. Chem. Chem. Phys.* **2005**, *7*, 3297.
(45) (a) van Wuellen, C. *J. Chem. Phys.* **1998**, *109*, 392. (b) van Leuthe, E.; Baerends, E. J.; Snijders, J. G. *J. Chem. Phys.* **1993**, *99*, 4597. (c) van Lenthe, E.; Baerends, E. J.; Snijders, J. G. *J. Chem. Phys.* **1994**, *101*, 9783. (d) Pantazis, D. A.; Chen, X. Y.; Landis, C. R.; Neese, F. *J. Chem. Theory Comput.* **2008**, *4*, 908.
(46) Neese, F. *J. Phys. Chem. Solids* **2004**, *65*, 781.
(47) Pettersen, E. F.; Goddard, T. D.; Huang, C. C.; Couch, G. S.; Greenblatt, D. M.; Meng, E. C.; Ferrin, T. E. *J. Comput. Chem.* **2004**, *25*, 1605.